



## Article

# Spatial–Temporal and Driving Factors of Land Use/Cover Change in Mongolia from 1990 to 2021

Junming Hao <sup>1</sup>, Qingrun Lin <sup>1</sup>, Tonghua Wu <sup>2,\*</sup>, Jie Chen <sup>2</sup>, Wangping Li <sup>1</sup>, Xiaodong Wu <sup>2</sup>, Guojie Hu <sup>2</sup> and Yune La <sup>2</sup>

<sup>1</sup> School of Civil Engineering, Lanzhou University of Technology, Lanzhou 730050, China

<sup>2</sup> Cryosphere Research Station on the Qinghai-Tibet Plateau, State Key Laboratory of Cryospheric Science, Northwest Institute of Eco-Environment and Resources, Chinese Academy of Sciences, Lanzhou 730000, China

\* Correspondence: [thuawu@lzb.ac.cn](mailto:thuawu@lzb.ac.cn)

**Abstract:** During the past several decades, desertification and land degradation have become more and more serious in Mongolia. The drivers of land use/cover change (LUCC), such as population dynamics and climate change, are increasingly important to local sustainability studies. They can only be properly analyzed at small scales that capture the socio-economic conditions. Several studies have been carried out to examine the pattern of LUCC in Mongolia, but they have been focused on changes in single land types at a local scale. Although some of them were carried out at the national scale, the data interval is more than 10 years. A small-scale and year-by-year dataset of LUCC in Mongolia is thus needed for comprehensive analyses. We obtained year-by-year land use/cover changes in Mongolia from 1990 to 2021 using Landsat TM/OLI data. First, we established a random forest (RF) model. Then, in order to improve the classification accuracy of the misclassification of cropland, grassland, and built and barren areas, the classification and regression trees model (CART) was introduced for post-processing. The results show that 17.6% of the land surface has changed at least once among the six land categories from 1990 to 2021. While the area of barren land has significantly increased, the grassland and forest areas have exhibited a decreasing trend in the past 32 years. The other land types do not show promising changes. To determine the driving factors of LUCC, we applied an RF feature importance ranking to environmental factors, physical factors, socioeconomic factors, and accessibility factors. The mean annual precipitation (MAP), evapotranspiration (ET), mean annual air temperature (MAAT), DEM, GDP, and distance to railway are the main driving factors that have determined the distribution and changes in land types. Interestingly, unlike the global anti-V-shaped pattern, we found that the land use/cover changes show an N-shaped trend in Mongolia. These characteristics of land use/cover change in Mongolia are primarily due to the agricultural policies and rapid urbanization. The results present comprehensive land use/cover change information for Mongolia, and they are of great significance for policy-makers to formulate a scientific sustainable development strategy and to alleviate the desertification of Mongolia.

**Keywords:** land use/cover; Google Earth engine; random forest model; Mongolia



**Citation:** Hao, J.; Lin, Q.; Wu, T.; Chen, J.; Li, W.; Wu, X.; Hu, G.; La, Y. Spatial–Temporal and Driving Factors of Land Use/Cover Change in Mongolia from 1990 to 2021. *Remote Sens.* **2023**, *15*, 1813. <https://doi.org/10.3390/rs15071813>

Academic Editors: Yaqian He, Fang Fang and Christopher Ramezan

Received: 6 February 2023

Revised: 19 March 2023

Accepted: 23 March 2023

Published: 29 March 2023



**Copyright:** © 2023 by the authors. Licensee MDPI, Basel, Switzerland. This article is an open access article distributed under the terms and conditions of the Creative Commons Attribution (CC BY) license (<https://creativecommons.org/licenses/by/4.0/>).

## 1. Introduction

Land use/cover change (LUCC) is the result of the comprehensive action of natural objective conditions and human socioeconomic activities, and its formation and evolution process is affected by natural factors and human activities [1]. Over the past 30 years, global warming has enhanced global vegetation greenness and human activities have accelerated land degradation [2]. However, climate change has indeed aggravated desertification and land degradation, especially in the middle and high latitudes of the northern hemisphere [3]. Land use change has affected almost one-third of the global land area in just six decades (1960–2019) and, thus, desertification is around four times greater in its extent than previously estimated from long-term land change assessments [4]. The speed, scale, and spatial

scope of human changes to the Earth's surface have reached an unprecedented level [5,6]. At the same time, LUCC can affect the global water and heat balance and biodiversity, thus affecting climate change and ecosystems at a regional and even global scale [7–9]. As an important input parameter of global climate models, LUCC directly affects the accuracy of the simulation and prediction of these models [10]. LUCC and its ecological impact have also become the focus of international research [11,12]. Therefore, understanding the causes, processes, and consequences of land use/cover change is crucial for a better understanding of the climate system, climate effects, and sustainable development [13].

The Mongolian Plateau (MP) lies in an arid and desert belt of the hinterland of Northeast Asia, within a horizontal crisscrossing zone of forest, grassland, and desert. Climate warming and human actions both have negative impacts on the land cover of Mongolia, and are accelerating land degradation [14]. Since 2002–2011, non-desertification and severe desertification areas have increased [15]. By 2016, approximately 72% of the land experienced desertification in Mongolia [16]. This increased to 76.8% in 2017, 24.1% of which experienced slight desertification, 29.8% experienced moderate desertification, 16.8% experienced severe desertification, and 6.1% was heavily degraded [17]. The land degradation of Mongolia has threatened the ecological environment and socioeconomic activities. Thus, it is of great significance to clarify the present situation, and the change processes and driving factors of land use/cover change in Mongolia.

In recent years, the long-term global dataset and various large-scale satellite data have been combined with statistics and machine learning methods to monitor and identify the LUCC of Mongolia and the entire MP. At present, the resolution of the existing global land cover dataset is from 1 km to 10 m, e.g., FROM-GLC (10–30 m, 2015, 2017, China) [18], Esri Land Cover (10 m, 2017–2021, ESA) [19], Globe land 30 (30 m, 2000, 2010, 2020, China) [20], Global Land Survey (30 m, 1975–2012, USGS) [21], Climate Change Initiative Land Cover V2 (300 m, 1992–2020, ESA) [22], and MODIS Land Cover Type/Dynamics (0.5–1 km, 2001–2020, NASA) [23]. These global land cover data can visualize spatial distribution, landscape patterns, and global land use trends. However, due to the limitation of samples and classification models, the results of different models in the same area are different [24,25]. Thus, fine classification and integration of land use/cover type on a regional scale has been mapped in Mongolia. On a local scale, the long-term land use/cover change is analyzed along the transect or economic corridor of the Mongolian plateau using Landsat TM and MODIS data from the 1990s to 2020s [26]. At regional scales, land use changes in Mongolia are mapped in combination with: (1) MODIS data and relevant statistical data in 1992–2005 [27]; (2) ESA 300 m resolution land cover data and TM data in 1970s and 2005 [28,29]; (3) TM data and survey data in 1997, 2007, and 2017 [30]; and TM and ETM+ using the NDVI thresholds method in 1990, 2000, 2010, and 2020 [31–33]. These studies can improve our understanding and provide new knowledge of land use/cover change in Mongolia over long periods. Generally speaking, the research on land use classification methods based on remote sensing is also expanding. Traditional remote sensing image classification methods, such as visual interpretation and statistics-based classification methods, have very simple algorithms [34,35]. However, the classification accuracy has reduced due to the phenomenon of foreign bodies. With the development of artificial intelligence algorithm classification methods, such as neural networks, decision tree classification, and the random forest method, the classification accuracy is higher than that of traditional methods, which is beneficial to a wide range of research results [36,37]. This type of black box operation is prone to overfitting. The classification and regulation tree (CART) method is applicable to a series of binary decisions formed in classification decisions based on human rules [38–40]. The random forest method has low classification error estimation for high-dimensional data [41,42]. Therefore, different methods are combined to improve the accuracy of remote sensing image classification [1,34,35].

The research on land use/cover change in Mongolia mainly focuses on forest decreasing, grassland degradation, urban expansion, and water body and lake change [37–41]. Global warming, logging, grazing, wind erosion, and human activity are considered as

the main driving factors [43–46]. Based on the national scale of Mongolia, most research is based on the land use status classification system, cropland, forest, built area, water area, barren land, and grassland [33,47]. They show that the land use in Mongolia is mainly cropland, accounting for 50.5% and increasing gradually, followed by bare land, accounting for 39.9% and gradually decreasing. In Northern Mongolia, due to the influence of climate change, forest area has gradually decreased by 5.4% and degenerated into grassland, and glaciers have turned into water bodies [46,48]. In the past ten years, under the influence of animal husbandry and socio-economic transformation, the area of barren land has decreased by 16.9% and the area of grassland has increased by 17.8% [45,49]. The change of built area is mainly in the Ulaanbaatar, with an area increase of 140%. The latest national-scale research is more than 10 years old [33,48,50], and there are no long-series data available for year-by-year comparison. However, the large data span and lack of continuous data have seriously affected the scientific understanding of the influencing factors and leading factors of land use/cover change in Mongolia.

Therefore, we mapped the land use/cover of Mongolia year-by-year from 1990 to 2021 based on Landsat TM/OLI and the random forest method, and then analyzed the patterns of land use change and driving factors. To improve the classification accuracy, a CART decision tree algorithm (CART) was developed. The aim of this study was to better measure the patterns and rates of the land use change in Mongolia and understand the influence factors.

## 2. Materials and Methods

### 2.1. Study Area

Mongolia is located in north-central Asia and belongs to an arid desert belt (Figure 1). It has an obvious continental climate with four distinct seasons. The average annual temperature was about 1.2 °C and increased by about 0.5 °C during 1998 to 2021 [51]. Annual precipitation rarely exceeds 400 mm and is typically much lower in the south and central desert and steppe regions. In the Gobi Desert, annual rainfall is only 40 mm [52]. The average altitude is 1580 m and the land use/cover types show transitional changes in forest, grassland, and barren land from high latitude to low latitude. The area of Mongolia is 1.56 million. According to the relevant statistics, grassland is the main type of land, accounting for about 59%, followed by bare land, which accounts for 20.8% [53]. At present, due to global warming and increased evaporation, a large number of rivers have dried up, the soil types have obviously changed, the ecological environment is more fragile, and desertification and other disasters are more likely to occur [54].

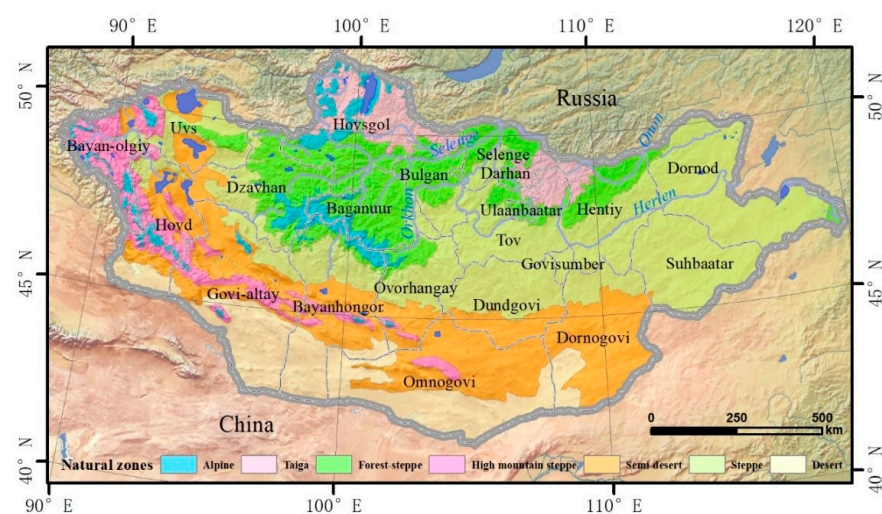


**Figure 1.** Location and natural features of Mongolia. The topographic base map was from [55].

## 2.2. Data Source

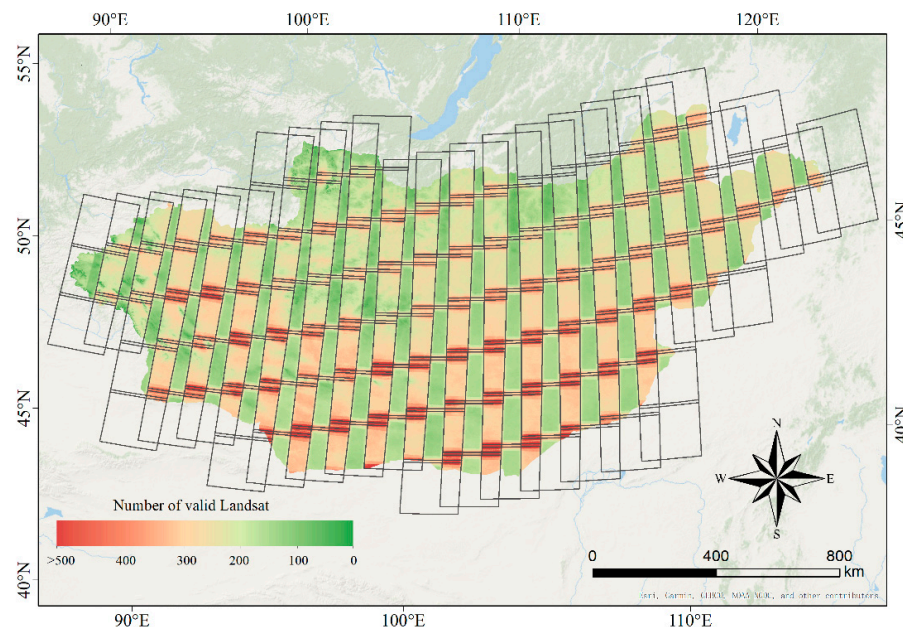
The types of land use in Mongolia referred to a previous study [56] and the international general LUCC standard (GB/T21010-2017) [57]. We classified the land use types into cropland, forestland, built area, water, barren land, and grassland. The Google Earth Engine (GEE) platform provided the possibility for large-scale remote sensing data processing and factors analysis [58]. The images from June to September were selected in GEE as data sources for 1990–2012 from Landsat 5 TM and for 2013–2021 from Landsat 8 OLI. They were preprocessed by geometric correction and atmospheric correction. Based on the study area, the high-quality remote sensing images were screened in GEE [59]. We found that there were at least 3 images in the same area. Then, median synthesis using a quality assessment band (OA) was used to screen the images with a cloud cover of <20% [60].

The driving factors of LUCC were selected based on a previous study and native environment. A previous study in Mongolia demonstrated that the MAAT, MAP, and ET are the key influencing factors of LUCC [61]. The influence of temperature on plant growth is comprehensive. It is not only an important condition for plant growth and development, but it also affects the growth cycle and greening period of cropland, pasture and forest vegetation, and the migration of the forest line [62–64]. Water is a critical limiting factor in arid and semiarid grassland areas and influences the land use type and regional climate [65,66]. The precipitation increasing by about 100–200 mm can alter the vegetation cover of the desertic Gobi [67]. The ET is related to a number of ecosystem processes, including photosynthesis, soil moisture, and latent heat transfer, and it plays an important role in the process of LUCC [68,69]. Human activities, as an influencing factor, have inhibited forest regrowth by fire or grazing [70]. The socioeconomic factors that are often considered are GDP and demography factors [71–73] due to national development policy and urbanization expansion. At the same time, Mongolia is dominated by herding activities. The increase in human activities and the development of animal husbandry on land degradation mainly influence the changes in grassland and built areas [70,74,75]. Thus, four types of influencing factors were selected: environmental factors, physical factors, socioeconomic factors, and accessibility factors. The factors were MAAT, MAP, ET, DEM, slope, aspect, GDP, population, livestock, distance to road, and distance to railway. (1) The environmental factors, including the mean annual air temperature (MAAT), the mean annual precipitation (MAP), and evapotranspiration (ET), were available from NOVA and PML\_V2 at a resolution of 30 m. (2) The physical factors included a digital elevation model (DEM) and the slope and aspect factors. A 30 m DEM was produced using SRTM-V4.1 by NASA. Based on the DEM, the terrain factors were extracted to obtain the corresponding slope and aspect. The aspect value range was 0–360°. (3) The socioeconomic factors comprised population, GDP, and livestock. The socioeconomic data were collected by province from the National Bureau of Statistics of Mongolia. Then, we converted the data into a raster dataset. (4) The accessibility factors, such as the distance to main roads (Dis\_road) and distance to railways (Dis\_railway), were obtained from the GRIP website. The GRIP dataset consisted of a global vector road dataset and a road density raster dataset at a resolution of 8 km. The accessibility variables were calculated by Euclidean distance in ArcGIS.

Table 1 provides detailed descriptions of these variables with their corresponding references. Figure 2 shows the availability of the Landsat images. Each dataset was generated as a layer in the ArcGIS environment and converted into a 30 × 30 m grid for model-fitting (Figure 3). The coordinate system was from a WGS-84, Baltic Sea level, and UTM projection (an official and unique coordinate system in Mongolia) on 28 January 2009 at a resolution of N28. See ref [76] for the coordinates.

**Table 1.** Data source description (All data accessed on 1 January 2022).

	Data Type	Time	Data Sources	Data Website Address
Image data	Landsat 5 (TM)SR	1990–2012	USGS	<a href="http://www.usgs.gov">www.usgs.gov</a>
	Landsat 8 (OLI)SR	2013–2021	USGS	<a href="http://www.usgs.gov">www.usgs.gov</a>
	DEM	2000	NASA	<a href="https://srtm.csi.cgiar.org">https://srtm.csi.cgiar.org</a>
	Land use/cover	2000–2020	GlobeLand30	<a href="http://www.globallandcover.com/">http://www.globallandcover.com/</a>
Basic geographic data	Livestock, Population	1990–2020	National Bureau of Statistics of Mongolia	<a href="http://en.nso.mn">http://en.nso.mn</a>
	ET	1990–2020	PML_V2, REA ET	<a href="http://poles.tpdc.ac.cn/zh-hans">http://poles.tpdc.ac.cn/zh-hans</a>
	GDP	2000–2021	National Bureau of Statistics of Mongolia	<a href="http://en.nso.mn">http://en.nso.mn</a>
	Road	1990–2021	GRIP global roads database	<a href="http://www.globio.info/download-grip-dataset">www.globio.info/download-grip-dataset</a>
	MAAT, MAP	1990–2021	NOVA	<a href="http://www.ncei.noaa.gov">www.ncei.noaa.gov</a>
	Land use/cover area	1990–2021	Mongolian Statistical Yearbook, CAS	<a href="http://1212.mn">http://1212.mn</a>

**Figure 2.** Effective number of Landsat images (cloud cover below 20%) of Mongolia from 1990 to 2021.

### 2.3. Extraction of Land Use/Cover Type

Our study attempted to develop a long-term land use extraction model for Mongolia. The extraction of land use/cover types with higher accuracy was carried out in the following four steps:

#### Step I. Data pre-processing

In this study, we selected Landsat bands (1~7) for the classification (Table S1), e.g., blue, green, red, near-infrared, short-wave infrared (SWIR\_1/2), and one thermal infrared (TIR) band. Further, surface bio-physical parameters, such as the normalized difference vegetation index (NDVI), the bare soil index (BSI), the normalized difference moisture index (NDWI), and the normalized building index (NDBI) were extracted. Finally, multi-bands imagery with 12 bands was produced for the image classification. The formulas are as follows:

$$NDVI = \frac{NIR - R}{NIR + R} \quad (1)$$

$$BSI = \frac{\rho(SWIR + R) - \rho(NIR + B)}{\rho(SWIR + R) + \rho(NIR + B)} \quad (2)$$

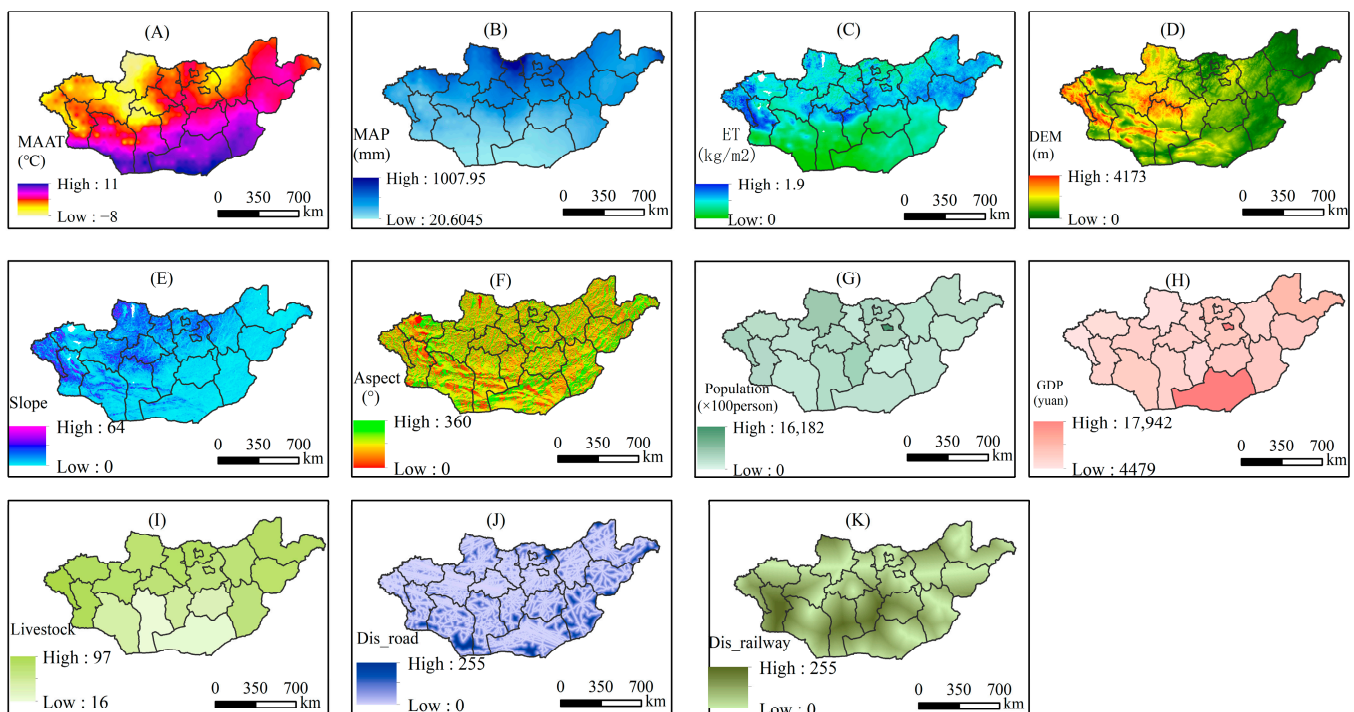
$$NDBI = \frac{SWIR - NIR}{SWIR + NIR} \quad (3)$$

$$MNDWI = \frac{G - MIR}{G + MIR} \quad (4)$$

where  $NIR$ ,  $MIR$ ,  $G$ ,  $R$ ,  $B$ , and  $SWIR$  are the reflectance values of the near-infrared band, the mid-infrared band, the green band, the infrared band, the blue band, and the short-wave infrared band, respectively.

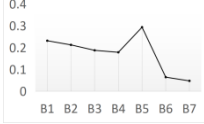
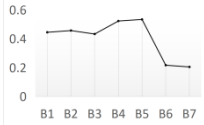
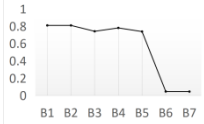
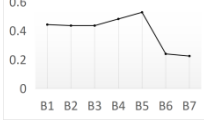
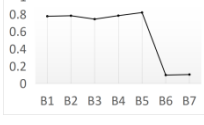
### Step II. Creation of training and testing samples

Accurate classification is a challenging task, especially with the confusion over the various spectral values such as for barren and built area land. The high-quality training samples and verification samples are needed for feature classification in RF. Therefore, we constructed a year-by-year sample library using visual interpretation in GEE. We used the function (`ee.ImageCollection`) on the GEE platform to display the Landsat images year by year. Then, the samples of each period in this study area were obtained by visual interpretation. GEE automatically extracted band information of different land use types to generate a sample library. The incorrect samples included in the different land types were deleted by the spectral characteristic curves, which were obtained with the mean band curve (Table 2). Finally, more than 2000 samples were selected from each year to establish a sample library. The sample types included cropland, forest, built area, water, barren land, and grassland. Then, 70% of the sample points were used as training samples for training classifiers and 30% as verification samples for accuracy verification [77,78].



**Figure 3.** Spatial distribution of driving force variables for land use changes between 1990 and 2021 in Mongolia. (A) MAAT, (B) MAP, (C) ET, (D) DEM, (E) slope, (F) aspect, (G) population, (H) GDP, (I) Livestock, (J) distance to road, (K) distance to railway.

**Table 2.** Characteristics of land use types.

ID	Land Type	Characteristic	Image Map	Spectrum Curve
1	Cropland	Land mainly planted with crops, including other economic trees		
2	Forest	Coverage > 30%, mainly including arbors, bamboos, and other plants		
3	Built area	Urban residential land, residential land, transportation facilities, and other buildings		
4	Water	Natural lakes, depressions, rivers, and artificial water conservancy		
5	Barren	Desert, rock, bare, Gobi, sandy land, and other areas with low vegetation coverage		
6	Grassland	Coverage > 15%, including desert grassland, meadow grassland, prairie, and other areas		

### Step III. Random forest

Random forest algorithm was widely used in land use/cover classification. Its basic principle is to construct a set of decision tree classifiers, and each decision tree will give a classification choice. The problem of decision tree over-fitting was improved by the voting mechanism of multiple decision trees, the majority voting mechanism strategy was used to obtain the final output [79], and bootstrap aggregation was used to modify the sample distribution, improving the generalization ability [80]. For the RF, all the training data were placed in a black box and then randomly picked to train the model [81]. Compared with other machine learning methods, the RF classification algorithm has better robustness and can run effectively on large datasets [82]. Moreover, some scholars have achieved excellent research results by using the RF algorithm on GEE to classify land use [83,84].

Land use/cover was performed by using the `ee.smileRandomForest` function in GEE API, which only needs to determine two parameters: the number of classification trees and the number of characteristic variables input when nodes splitting [83,85]. In order to prevent over-fitting, we tested the number of trees with a threshold of 50 trees. When the number of trees exceeded 100, the model trended to stable. Therefore, 150 trees were finally selected for RF classification, and 6 random variables were selected from the best split when each tree grows.

### Step IV. Post-processing of classification

By analyzing the land use/cover classification of the RF, we found that the barren land, built area, grassland, and cropland were misclassified. Therefore, we post-processed the classification results to improve the accuracy of land cover classification. Firstly, we divided the areas that may have been built area or cropland using the CART (Classification and Regression Trees) decision-making method in GEE. Then, the divided areas were

further classified by RF through the constructed sample library. The CART method is often applied to land use classification [86]. The CART method usually includes a selection of variables, decision tree generation, and pruning of the decision tree [87]. The accuracy of the analysis can be improved by observing the classification results when modifying the node threshold of the decision tree or optimizing the training data [88]. We found that the cropland was characterized by NDVI ranging from 0.25 to 0.45, while the NDBI values of the built areas were all greater than 0.1, and the BSI value was greater than 0.12. Thus, we constructed a CART decision tree based on the thresholds of the NDVI, NDBI, and BSI. We briefly divided the three areas using the CART. First, the cropland and grassland were divided by the NDVI, in which  $0.25 < \text{NDVI} < 0.45$  was classified as the first partition (including all croplands and part-grasslands).  $\text{NDBI} > 0.1$  and  $\text{BSI} > 0.12$  were defined as the second partition (including all built areas and part-barren). Other types of land were defined as the third partition. Finally, we used the RF method to reclassify the land use/cover types of the first and second partitions independently, and updated this part of the area using the `imagePlough.updateMaskd` function in GEE to obtain the final land use classification result.

In addition, we calculated the influence of each variable on the heterogeneity of the observed values at each node of the classification tree by using `MeanDecreaseGini` on the R platform [89]. The greater the value, the greater the importance of the variable, so we used `MeanDecreaseGini` to verify the importance of different factors to land use types and rank them. We used the function of `Importance()` in the R statistical software package to calculate the `MeanDecreaseGini` value between each driving factor and land use type. Finally, visual representation of the importance of variables was carried out by using the `varImpPlot` function in the R statistical software package.

#### 2.4. Accuracy Evaluation

A confusion matrix is often used to evaluate the accuracy of each land cover type [90]. For single-date maps, a confusion matrix was built in GEE to evaluate the accuracy of LUCC classification, and then the overall accuracy (OA), producer accuracy (PA), user accuracy (UA), and Kappa coefficient of the quantitative indicators were calculated [85]. UA is the probability that a value predicted to be in a certain class really is that class. PA refers to the probability that a value in a given class was classified correctly. For the change of land use type, the accuracy was evaluated with the method of [91]. We selected the samples of the changed areas considering 18 reporting themes in 6 land use/cover types on 2015 and 2021 (Table S2). Then, the change accuracy was analyzed by three indexes: land use gain, loss, and no change. Gain refers to some type of increase, loss refers to some type of decrease, and no change refers to no change during the study period. For example, between 2015 and 2020, cropland loss means a change from cropland to any other class, cropland gain means a change to cropland from any other class, and no change means no change in cropland during this period. Then, the confusion matrix for the accuracy of the change of land use types in two periods was calculated. Moreover, five typical areas in two existing land use products (Google Earth and GlobeLand30) were selected to evaluate the spatial distribution of classification [87]. The related formulas were as follows:

$$UA = \frac{X_{ij}}{X_j} \times 100\% \quad (5)$$

$$PA = \frac{X_{ij}}{X_i} \times 100\% \quad (6)$$

$$OA = \frac{S_d}{n} \times 100\% \quad (7)$$

$$Kappa = \frac{p_o - p_e}{1 - p_e} \quad (8)$$

where  $X_{ij}$  is the observed value of the  $i$ th row and the  $j$ th column in the confusion matrix;  $X_i$ ,  $X_j$  represent the marginal totals of the  $i$ -th row and the  $j$ -th column, respectively;  $X_{ii}$  represents the observed value of the  $i$ -th row and the  $i$ -th column in the confusion matrix;  $p_o$  equals  $OA$ ; and  $p_e$  is the ratio of the product sum of the actual sample number of each class and the predicted sample number of each class to the square of the total sample number  $n$ .

### 2.5. Land Use/Cover Change Dynamic Degree

Based on the statistics of the area changes in different land use/cover change types in each grid, the dynamic degree model and conversion matrix were used to analyze land use change processes. The dynamic degree model developed by [92] was divided into single and comprehensive models to describe the expansion and shrinkage of types of land use. The single land use dynamic degree model ( $K$ ) can quantity one land use type during a specified period, while the comprehensive land use dynamic degree ( $LC$ ) was used to characterize the rate and amplitude of land use change in the study area. The formulae are as follows:

$$K = \frac{LU_a - LU_b}{LU_a} \times \frac{1}{T} \times 100\% \tag{9}$$

$$LC = \left[ \frac{\sum_{i=1}^n \Delta LU_{i-j}}{2 \cdot \sum_{i=1}^n \Delta LU_i} \right] \times \frac{1}{T} \times 100\% \tag{10}$$

Here,  $LU_a$  and  $LU_b$  are the areas of this land use type in the initial year ( $a$ ) and end year ( $b$ ) of the study period;  $LU_i$  is the area of the  $i$  types;  $\Delta LU_{i-j}$  is the area of the  $i$ -th type that is converted to another type;  $n$  is the number of types; and  $T$  is the study period, which is five years.

We used ArcGIS spatial analysis to superimpose the land use types in different periods, obtain the structural characteristics and transfer the matrix of land use change, and show the transformation relationship between different land use types in two periods in the form of charts.

In brief, based on the Landsat dataset and the Google Earth Engine platform (GEE), we took the random forest as the main body of the classifier and combined the regression trees (CART), obtained the land types of Mongolia over nearly 30 years, and analyzed the patterns and dynamic and driving forces. The brief details of the methodology applied in this research are presented in Figure 4.

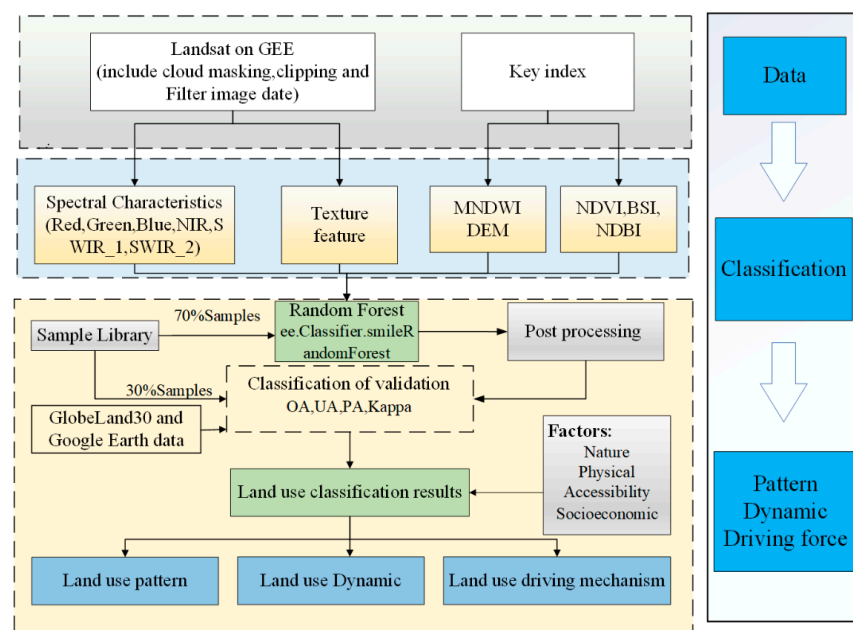


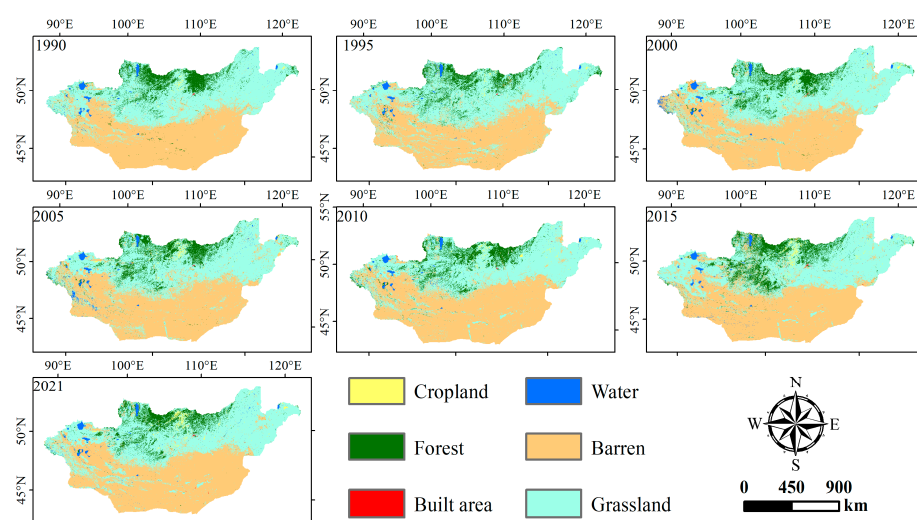
Figure 4. Methodological flowchart for this study.

### 3. Result

#### 3.1. Land Use/Cover Pattern

Land use/cover in Mongolia is classified into six types: cropland, forest, built area, water, barren land, and grassland. Grassland, barren land, and forest areas are the main land use/cover types in Mongolia.

The spatial distribution of land use/cover in Mongolia from 1990 to 2021 is shown in Figure 5 and Figure S1, and Table 3. Generally speaking, the area of grassland is the largest, accounting for more than 43% of the national area mainly in the central and northern regions of Mongolia. Barren land occupies more than 40%, mainly as arid barren land and desert distributed in southern Mongolia. Sporadic grassland is distributed in the basins and Gobi areas. More than 7% is forest land, mainly distributed in the north of the Kent-Hang'ai Mountain. The water bodies mainly comprise plateau lakes. The cropland and built areas are the smallest, making up about 1% of the whole country. Generally speaking, the grassland, barren land, and forest areas in Mongolia are the most widely distributed types, accounting for more than 95%. The land use/cover type pattern from north to south is a transitional distribution of forest–grassland–barren land.

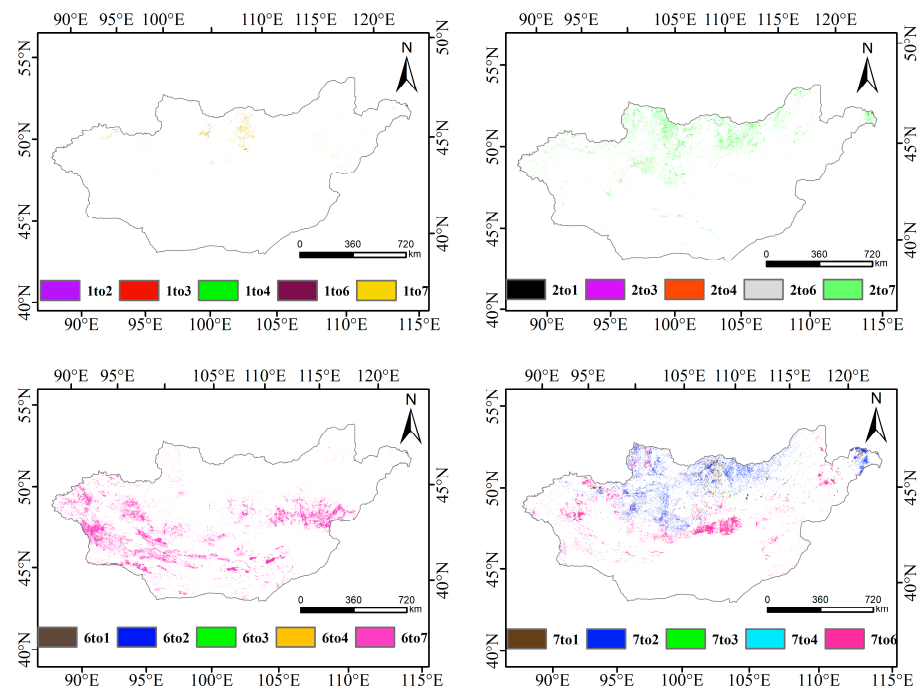


**Figure 5.** Spatial distribution of land use type in Mongolia from 1990 to 2021.

To intuitively reflect the spatial characteristics of LUCC, we used the grid calculator of ArcGIS to calculate the spatial distribution map of mutual transformation between different land use/cover. The land use change pattern in Mongolia from 1990 to 2021 is shown in Table 3 and Figure 6. We estimate that  $27.5 \times 10^4 \text{ km}^2$  of the land surface in Mongolia, accounting for 17.6%, changed at least once among the six land categories from 1990 to 2021. The grassland, water, cropland, and built areas exhibited a growing trend, while the barren land and forest areas decreased. Among all types, the amplitude of land use change was the smallest for forest land and the largest for built areas. The area of barren land decreased by  $6.2 \times 10^4 \text{ km}^2$ , mainly in central Mongolia. The forest area decreased by  $0.5 \times 10^4 \text{ km}^2$ , mainly in the Selenge Valley in northern Mongolia. Meanwhile, grassland and water area increased. The grassland increased by  $6.6 \times 10^4 \text{ km}^2$ , mainly in eastern Mongolia. The water area increased by  $1007 \text{ km}^2$ , which was mainly related to the changed area of lakes on the plateau. The area with the least amount of change was the built area, but it increased dramatically from  $499 \text{ km}^2$  to  $1242 \text{ km}^2$ , representing approximately twice the growth rate of the other areas. On the time scale, taking 2005 as the boundary, the barren area first showed an increasing and then decreasing trend. In addition, compared to 1990, the increase in barren land mainly occurred in the East Gobi and North Donogovi provinces. The change in the grassland area first showed a decreasing and then increasing trend, and the increase in grassland mainly occurred in northern Mongolia, particularly in the Selenge prefecture.

**Table 3.** The areas of different land use types in Mongolia from 1990 to 2021.

	1990		1995		2000		
	Area (km <sup>2</sup> )	Proportion (%)	Area (km <sup>2</sup> )	Proportion (%)	Area (km <sup>2</sup> )	Proportion (%)	
Cropland	11,985	0.73	9972	0.60	11,881	0.71	
Forest	129,645	7.93	141,098	8.56	120,431	7.36	
Built area	499	0.03	539	0.03	651	0.04	
Water	16,462	1.01	16,989	1.03	17,872	1.09	
Barren	723,413	44.25	696,490	42.26	770,983	47.14	
Grassland	752,708	46.05	783,298	47.52	710,830	43.47	
2005		2010		2015		2021	
Area (km <sup>2</sup> )	Proportion (%)	Area (km <sup>2</sup> )	Proportion (%)	Area (km <sup>2</sup> )	Proportion (%)	Area (km <sup>2</sup> )	Proportion (%)
10,901	0.67	10,761	0.66	11,703	0.71	12,720	0.77
116,992	7.15	116,854	7.15	129,406	7.91	124,524	7.61
647	0.04	800	0.05	1037	0.06	1242	0.08
16,649	1.02	16,425	1.01	17,860	1.09	17,469	1.07
777,381	47.50	754,526	46.10	725,936	44.35	661,066	40.40
714,031	43.62	737,004	45.03	751,015	45.88	819,205	50.07

**Figure 6.** Land use change in Mongolia from 1990 to 2021; 1—cropland, 2—forest, 3—built area, 4—water, 5—barren, and 6—grassland.

### 3.2. Land Use/Cover Change Dynamic

In order to explain the degree of LUCC, the comprehensive and single land use dynamic degrees were calculated on the classification scale (Figure 7A). Over the past 32 years, the comprehensive land use dynamic degree had an N-shaped trend. Three stages of change were presented. It increased significantly from 0.36% to 0.88% in 1990–2000, then dramatically reduced to 0.09% in 2000–2005. Subsequently, the dynamic degree increased continuously, and the land use/cover change dynamic were 0.24%, 0.29%, and 0.61%. Considering the dynamic degree of single land use, the built areas showed an overall growth tendency. It began to increase substantially after 2005 and reached a peak of 4.94%

in 2010–2015. Cropland decreased in 2005 and then increased. The forest area decreased the most from 1995 to 2000 and gradually increased after 2010. The water area was in a state change, with the biggest change from 1995 to 2000 showing an increasing trend. The barren land increased first and then decreased, with the largest decrease in 2015–2021. The grassland decreased the most in 1995–2000, and the growth rate was the largest in 2015–2021. Generally speaking, the comprehensive land use dynamic degree of Mongolia over the past 32 years showed an upward trend before 1990–2000, and a downward trend from 1995 to 2010. It showed an upward trend from 2005 to 2021. In terms of land types, the increase in built areas began to increase after 2005, reaching a maximum in 2010–2015; cropland also began to increase, especially after 2010.

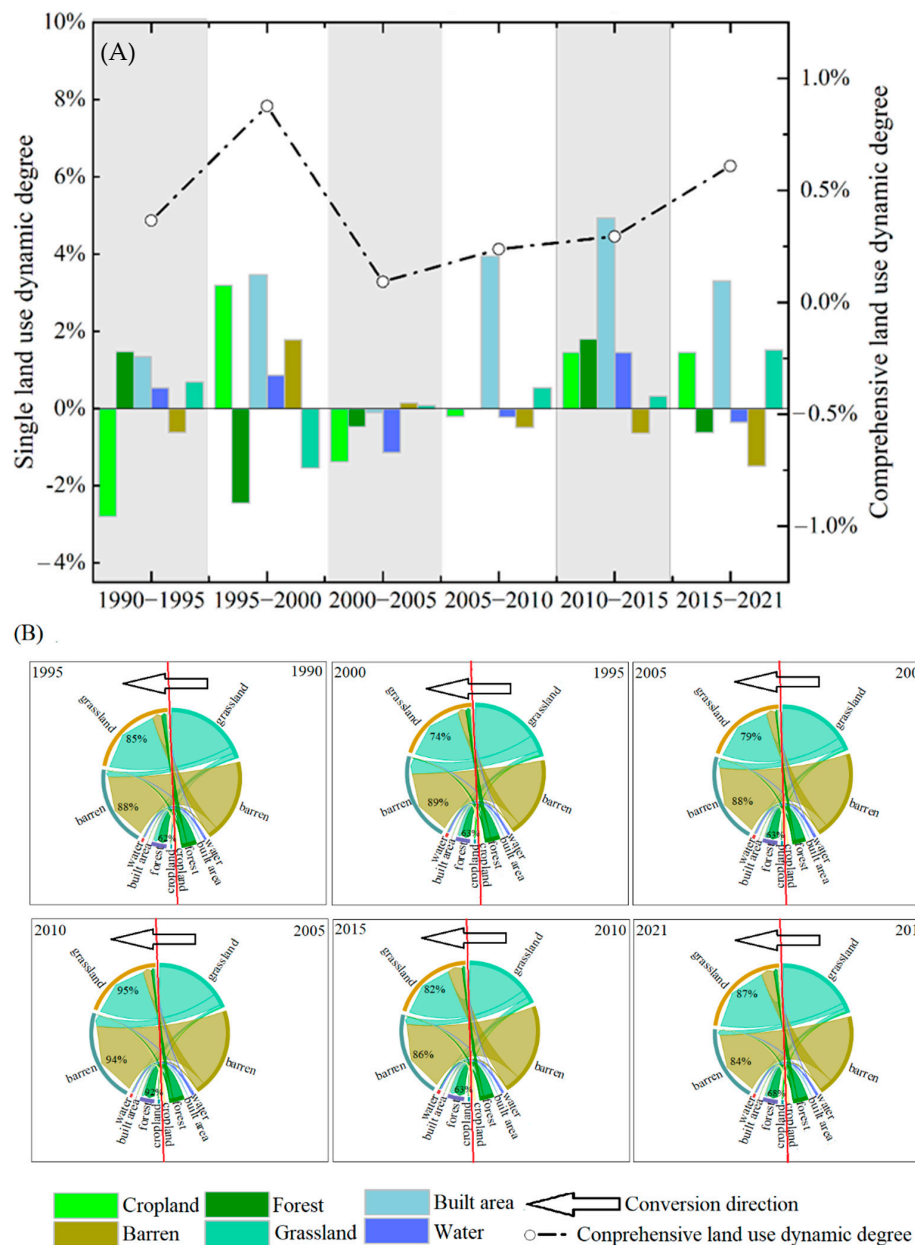


**Figure 7.** Dynamic degree (A) and transfer matrix Sankey diagram (B) of land use/cover change in Mongolia from 1990 to 2021. Note: In the figure, the land use change in different years is divided by red lines, the arrow direction represents the transfer direction of land use types, and the percentage indicates how many land use types have not changed during the two periods.

In order to reflect the specific situation of mutual transformation among the different land use/cover change types, we determined the area conversion of each type in each period using a transfer matrix (Figure 7B). It can be seen that, over the past 32 years, area change in Mongolia was mainly a mutual transformation between grassland and barren land. From 1995 to 2000, grassland was mainly transformed into barren land in 2010–2015, and the opposite occurred from 2010 to 2015. The final statistics show that from 1990 to 2021, the area of barren land converted into grassland was  $1.1 \times 10^5 \text{ km}^2$ . Other land types were also transformed, but this was not obvious because of their small size.

In conclusion, over the past 32 years, the comprehensive dynamic degree in Mongolia showed an N-shaped trend, and 2005 was a turning point. Built area changed dramatically. Particularly from 2010 to 2015, there was obvious mutual transformation between grassland and barren land, and grassland increased and barren land decreased, which indicates that desertification control in Mongolia achieved good results.

### 3.3. Influencing Factors of LUCC

Based on the R platform, we used the RF algorithm to rank the relative importance of 11 driving factors on land use/cover change (Figure 8). It can be seen that the MAAT, ET, and MAP were the main driving factors in the past 32 years, and the sum of the relative importance of these three categories was more than 50%. As far as environmental factors are concerned, the relative influence of the MAAT, ET, and MAP is high. The environmental factors were the most important factors affecting the land use/cover change types. In terms of the physical factors, the DEM had an obviously high influence, and most of the forests were distributed in 1000–2000 m a.s.l., while the grassland was mainly located above 3000 m a.s.l. in southern Mongolia. Considering the socioeconomic and accessibility factors, the Dis\_railway, GDP, and livestock factors had great influence on the LUCC, which is mainly related to policy and lifestyle in Mongolia.

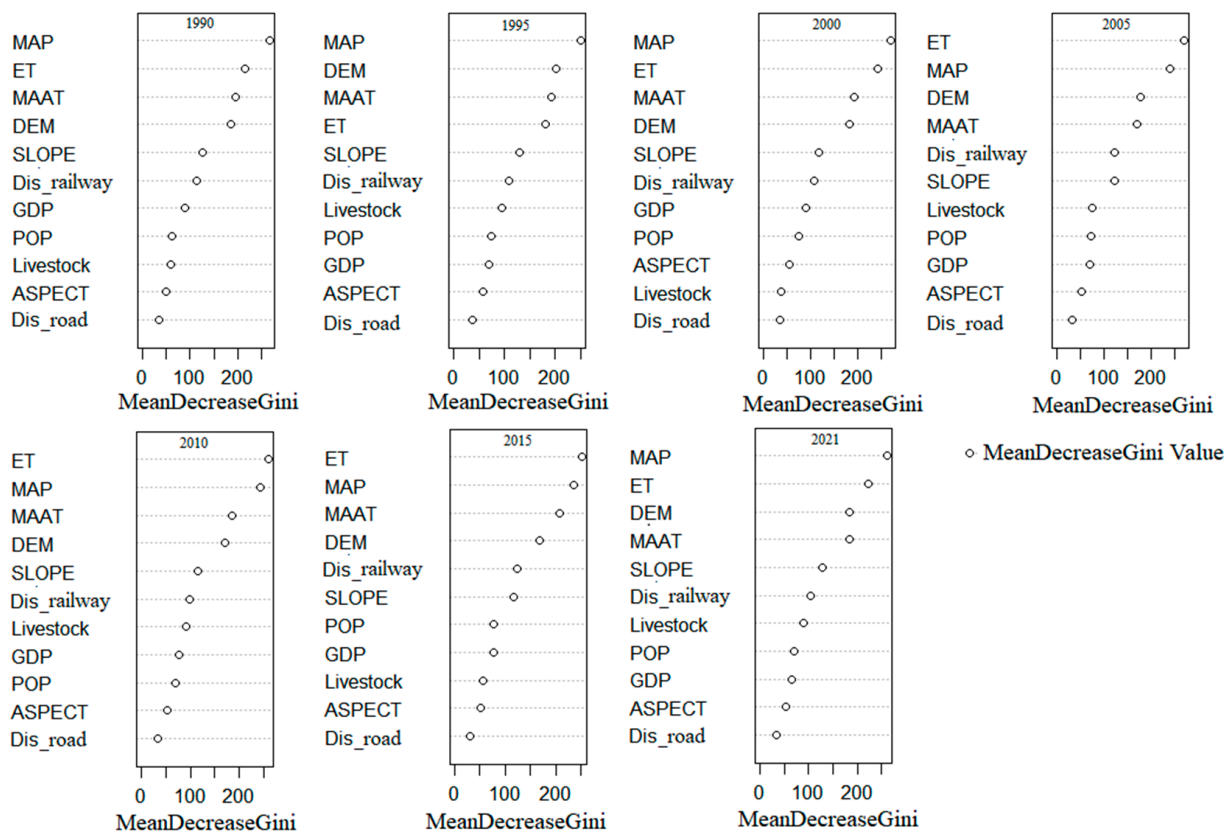


Figure 8. Relative importance (MeanDecreaseGini) of the land use/cover change driving factors.

## 4. Discussion

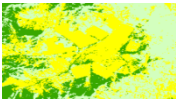
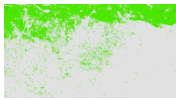
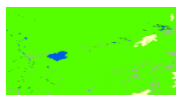
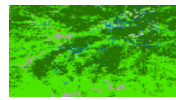
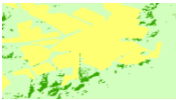
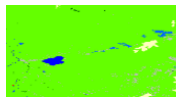
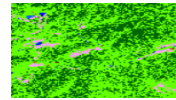
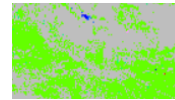
### 4.1. Validation

Based on the RF, we calculated the confusion matrix to evaluate the accuracy of each land type. According to the accuracy of the producers and users, the random forest classification had the highest accuracy for forests, water, and barren land. On the whole, the overall accuracy rate and kappa coefficient were more than 76% and 0.7 (Table 4 and Table S2), which met our research needs. Comparing the Google Earth and GlobeLand30 data [93] (Table 5), it was found that the patterns of different types were similar, while there were some errors between the cropland and water land types, which may have been related to different image dates or image sensors. The difference between the PA and UA can be seen in Table 4. This is because the image features of cropland are similar to those of grassland [94]. Moreover, cropland changed greatly, and its abandonment also led to a greater degree of fragmentation, which interferes with the division of these two land types. Meanwhile, we compared the recent land use areas in Mongolia. Our results are basically consistent with those of [32] and different from those of [48], especially for cropland, grassland, and barren land (Table 6). This may be related to the effect of different approaches, as [48] used the NDVI threshold method to identify the land types, and the threshold value is affected by many uncertain factors, e.g., times, images, and places.

**Table 4.** Accuracy verification.

LUCC Type	Accuracy Type	1990	1995	2000	2005	2010	2015	2021
Cropland	PA (%)	74	62	63	59	64	59	70
	UA (%)	94	94	92	94	94	93	94
Forest	PA (%)	80	75	78	75	75	82	86
	UA (%)	88	83	89	84	85	90	85
Built area	PA (%)	66	59	77	61	61	60	70
	UA (%)	100	100	95	100	100	100	98
Water	PA (%)	93	93	92	93	94	89	89
	UA (%)	98	97	96	97	95	94	99
Barren	PA (%)	88	83	87	89	89	85	83
	UA (%)	95	89	84	88	89	88	91
Grassland	PA (%)	91	88	83	87	87	87	87
	UA (%)	73	66	68	68	69	67	71
OA (%)	--	84.63	78.32	80.01	79.94	80.63	79.83	82.42
Kappa	--	0.7677	0.7127	0.7382	0.7349	0.7445	0.7332	0.7689

**Table 5.** Verification of classification results.

Data Source	Classification Result Comparison				
Google Earth					
Our paper					
GlobeLand30					

**Table 6.** Comparison of land use changes in Mongolia and other regions.

Regions	Year	Interval	Land Use Change Rate (%)						Reference
			Cropland	Forest	Grassland	Water	Built	Barren	
Mongolia	1990–2021	1	+8.5	−2.5	+8.5	+7.1	+156.1	−8.6	This paper
Mongolia	1990–2020	10	−27.0	−5.4	+18.4	−8.1	+150.7	−15.2	[48]
Mongolian Plateau	1990–2020	10	+4.9	−1.5	+10.5	−0.6	+47.2	−13.4	[32]
Inner Mongolia	2000–2015	5	−0.2	−1.0	+0.7	+2.3	+22.5	+0.4	[95]
Central Asia	1995–2015	10	+16.1	−0.1	−3.0	−0.2	+223.5	−4.0	[96]
North and West Africa	1985–1995	10	+3.6	−1.5	+64.4	+82.7	+169.4	+1.2	[97]
Global	2001–2012	12	−0.5	−1.2	+2.0	+1.0	−0.1	−6.2	[98]

Note: “+” means an increasing trend, and “−” means a decreasing trend.

At present, the evaluation of error and uncertainty of land use data also included change accuracy [92]. We verified the change accuracy of land cover types, taking 2015 and 2021 as an example (Table S4). It was shown that the no-change-reporting themes had higher agreement and that the change-reporting themes had lower agreement. During the 2015–2021 change periods, forest gain UA was between 80% and 86%. Barren loss PA approached 90.95%. PA for most of the remaining reporting themes ranged from 70% to 80% with agriculture gain and water gain being exceptions, with PA below 65%. The change accuracy may be related to the fragmentation and distribution of land types. The UA of water and grassland was lower; the UA of most of the remaining reporting themes ranged from 70% to 80%. Obviously, the no-change themes had higher consistency. The research showed that UA and PA may be higher in homogeneous regions for the changing region, while the accuracy was lower in heterogeneous regions (such as a single isolated pixel) [86,93].

We selected numbers using parameter optimization. RF can accurately and robustly process high-dimensional and multicollinear data [94]. Over-fitting does not increase according to the number of trees in the RF model, but it tends to be stable with more trees [95]. Therefore, we took 50 trees as increments and finally chose 150 trees to participate in the classification. We improved the accuracy of the image classification using the CART method, but the image quality, natural environment, and dispersion rate may still have affected the accuracy of the classification, especially for the cropland and built area (Table 4 and Table S3). However, the spatial distribution of cropland in Mongolia is discrete. The distribution of cropland and grassland is mixed and led to misclassification. In addition, cropland and grassland have similar spectral characteristics in the growing season, which also affects the classification accuracy. A previous study also found that the classification accuracy of cropland fluctuated greatly compared to other types [96]. For example, the PA of cropland was different between 1990 and 1995, as seen in Table 4. The built land is also very discrete, which is similar to the spectral information of barren land, which also affects the classification accuracy, e.g., the PA and UA.

This method is generally used for large-scale land use classification research. However, the selection of images in different months of the growing season, the influence of cloud cover and the imbalance of sample points will still affect the accuracy. Additionally, solving the problem of land use/cover types with similar spectral characteristics and realize further fine classification is still the focus of current research.

#### 4.2. Reasons for Land Use Change

One of the significant factors leading to vegetation change in Mongolia is climate change [52]. Over the past 32 years, we found that the MAP and ET had the greatest influence on land types, followed by MAAT (Figure 8). We found that cropland in Mongolia only accounts for 1% of the whole country, which is closely related to the typical arid environment of Mongolia. The overall forest in Mongolia still shows a slight decreasing trend, and the proportion of grassland types is gradually increasing. This is consistent with the results of [33,48]. In Mongolia, the MAP in the growing period of plants has decreased

by 33 mm since 1961 [99]. The grassland changes in Mongolia are mainly due to global climate change [33]. Over the past 70 years, the MAAT in Mongolia has increased by 2.1 °C, resulting in an increased loss of soil moisture through evapotranspiration [100]. Meanwhile, the increase in temperature and the decrease in precipitation has led to a dry climate, which affects surface evaporation and plant growth. Although the significance of temperature was slightly lower, the change in temperature did have a greater impact on some areas [27]. Meanwhile, the special characteristics of LUCC are consistent with the regions in Mongolia with decreasing precipitation and increasing temperature [101].

Socioeconomic factors also play a key role in land use/cover change in Mongolia. After 1995, grassland in Mongolia showed a trend of degradation, which was mainly related to Mongolia's emphasis on economic development at that time (Figure 7 and Table 3). This is consistent with the results of [102] and may be related to the continuous advancement of privatization and overgrazing and the development of animal husbandry [103]. The concept of "development before governance" has had a profound impact on Mongolia and may have led to increasing built areas and decreasing cropland from 1990 to 2010, showing opposite trends [104,105]. In order to increase its GDP, Mongolia began to exploit mineral resources in large quantities and built railways to facilitate the transportation of resources, which caused great damage to the environment and, thus, had a great impact on land types [106]. Therefore, the significant influences of GDP and Dis\_railway on land use/cover types appear to have gradually increased. The implementation of the "Four Modernizations" policy in 2010 led to a sharp increase in the built areas of Ulaanbaatar.

Overall, it holds that the changes in Mongolia are restricted by natural factors such as climate, but they are also driven by policy and economic development.

#### 4.3. Analysis of the LUCC Pattern in Mongolia and Globally

To evaluate the land use/cover change in Mongolia, we summarized the global and regional land changes, such as the surrounding areas of Mongolia and some representative arid areas (Table 6). Globally, barren land and forest land show a decreasing trend. The area of barren land in arid areas such as Mongolia and the Mongolian Plateau has reduced significantly, and the same is true for the global barren land. These changes may be related to global greening [107,108]. However, at present, desertification is still a global phenomenon that cannot be ignored, as it will destroy global biodiversity and aggravate the occurrence of natural disasters [109]. Land use/cover change was the highest for built land and lowest for forest areas during the studied time period in Mongolia, Central Asia, and Africa. Forest land shows a continuous decreasing trend, especially in arid areas such as Mongolia and East Africa. During rapid urbanization in developing countries, the area of built land is greatly increased. According to the research presented here, the natural degradation of forest has exceeded deforestation, which poses a great threat to the natural environment [110]. Although the proportion of grassland has started to increase in Mongolia, this is mainly due to the implementation of a series of new policies and ecological projects by both the Chinese and Mongolian governments [111]. From the perspective of global change, desertification is still an urgent problem to be solved.

Generally speaking, global water and grassland areas show a growth trend, while barren land is decreasing, indicating that global desertification control has achieved initial results. Cropland areas have also begun to increase, but global forest degradation still needs to be solved. According to a regional analysis of East Africa and the Mongolian Plateau, although desertification control in arid and semi-arid areas has achieved results, it cannot be ignored, and forest degradation is still obvious.

The LUCC pattern in Mongolia shows an N-shaped trend and can be divided into three stages—declining in 1995–2005 and increasing in 1990–2000 and 2005–2021. Meanwhile, the dynamics of global land use/cover change show an upside-down V-shaped pattern, accelerating during 1960–2005 and decelerating from 2006 to 2019 [4]. This is contrary to the global land use/cover change processes outlined by [4] from 1995 to 2010. This may be related to policies, rapid urbanization, and climate change factors. The policy

and urbanization development in Mongolia have influenced the land use dynamic degree. Mongolia's urbanization started late, and its urbanization rate began to increase significantly after 2005 and 2015 [112]. However, the data show that since 2005, land use/cover change has started to rise, which is due to the global economic crisis; this has led to an increased demand for biofuels and minerals. Unlike other countries that depend on imports (EU, China), Mongolia started to exploit resources to speed up its development, which led to changes in land types to different degrees [113]. Regarding the food demand in Mongolia, global food production changed from agricultural technology intensification to global market and trade growth, especially in 1990 [114]. However, under the influence of the Four Modernizations policy and drought, cropland in Mongolia decreased by 21% from 1994 to 1999 [115]. Grassland restoration has mainly been due to the implementation of the Green Great Wall Project [116]. Due to the implementation of returning farmland to forests and grasslands, grasslands have been expanded from farmland, but from the results, most grassland area in Mongolia still comes from former forests and barren land. The results of this policy are consistent with those of [87]. Generally speaking, the recent implementation of environmental policy has been helpful to realize the sustainable development of grassland. Specifically, the grassland–barren land boundary has gradually recovered since 2010, and the grassland area has started to increase steadily.

Rising temperatures and decreasing precipitation have had a great influence on the land use/cover change in Mongolia [100]. In 1998, the climate of the Mongolian Plateau was identified as being at a turning point from wet to dry, which made Mongolia transition from a wet period to a more severe drought period [117], and the area of barren land increased between 1995 and 2000. After 2005, rainfall began to change from a downward trend to an upward trend [118]. According to the drought grade, the areas with a high frequency of severe drought (6–11%) are mainly located in southern Mongolia and central and western Mongolia. In addition, from 2001 to 2009, land degradation in Mongolia was frequent [119]. During 1990–2000, Mongolia experienced a turning point of rainy and arid years. The forest and grassland areas increased first and then decreased, and the land use/cover changed greatly. From 2000 to 2005, the grassland area remained relatively stable, and the change range of land use/cover in Mongolia decreased. After 2010, the barren area in Mongolia continued to decrease, the grassland area steadily increased, and the desertification process was effectively controlled. The conclusion drawn in this study studies are similar to the conclusions of [48].

## 5. Conclusions

In our study, we integrated the random forest method and a classification and regression tree model for identifying the land use/cover type in Mongolia between 1990 and 2021. By comparing the land use/cover change patterns and the dynamic and driving factors in different years, we determined the land use change and the significance of influencing factors on land use over the past 32 years. The results are as follows: (1) The grassland, barren land, and forest areas in Mongolia are the most widely distributed types, accounting for more than 95% of the land. (2) Over the past 32 years, 17.6% of the land surface changed at least once among the six land categories, and the land use dynamic degree had an N-shaped trend. (3) Grassland, water, cropland, and built areas exhibited a growing trend, while barren land and forest areas decreased. (4) The MAP, ET, and MAAT are the main environmental factors that determined the distribution and changes of land types, while Dis\_railway and GDP are the main socioeconomic and accessibility factors that influenced the change patterns of land use. Meanwhile, the physical environment also plays a key role.

Land use and land cover change are significant for a range of themes and issues central to the study of global environmental change and sustainable development strategy. It is widely acknowledged that a better understanding of land use dynamics over the next 30–50 years is central to the debate on sustainability. We mapped the land use change in Mongolia over the past 32 years at a resolution of 30 m and explained the spatial patterns

and change processes, which is valuable for understanding the change information and desertification of Mongolia and the Mongolian Plateau.

**Supplementary Materials:** The following supporting information can be downloaded at: <https://www.mdpi.com/article/10.3390/rs15071813/s1>, Figure S1: Spatial distribution of land use type in Mongolia from 1990 to 2021. The lack of land use type in 2012 due to the missing of remote sensing images; Table S1: Landsat5 and Landsat8 band parameters; Table S2: Reporting themes for accuracy results. Table S3: Verification of classification accuracy. Table S4: UA and PA of LUCC.

**Author Contributions:** J.H. and Q.L. were responsible for the conceptualization, methodology and writing of the original draft, J.C. and Y.L. were responsible for the methodology and data curation; W.L. and G.H. were responsible for data checking—review and editing; T.W. and X.W. helped with the editing and are responsible for the funding acquisition. All authors have read and agreed to the published version of the manuscript.

**Funding:** This research is supported by the National Natural Science Foundation of China (41961144021 and 32061143032), the CAS “Light of West China” Program (Granted to Tonghua Wu) and Educational the Technology Innovation Project of Gansu Province (2023CXZX-464).

**Data Availability Statement:** The data has not yet been completed online. Please contact the first or corresponding author if needed.

**Acknowledgments:** Thanks to the Shuttle Radar Topography Mission (SRTM), the National Bureau of Statistics of Mongolia, the NASA, USGS and NOVA Organization for their data support. We would also like to thank all the staff members of the Google Earth Engine and Google Colaboratory. Special thanks also to the reviewers and editors; your comments and suggestions have greatly improved the paper’s content.

**Conflicts of Interest:** The authors declare that they have no known competing financial interests or personal relationships that could have appeared to influence the work reported in this paper.

## References

1. Perminova, T.; Sirina, N.; Laratte, B.; Baranovskaya, N.; Rikhvanov, L. Methods for Land Use Impact Assessment: A Review. *Environ. Impact Assess. Rev.* **2016**, *60*, 64–74. [[CrossRef](#)]
2. Affeld, K.; Wisner, S.K.; Payton, I.J.; DeCáceres, M. Using Classification Assignment Rules to Assess Land-Use Change Impacts on Forest Biodiversity at Local-to-National Scales. *For. Ecosyst.* **2018**, *5*, 162–176. [[CrossRef](#)]
3. Stoerk, T.; Wagner, G.; Ward, R.E.T. Recommendations for Improving the Treatment of Risk and Uncertainty in Economic Estimates of Climate Impacts in the Sixth Intergovernmental Panel on Climate Change Assessment Report. *Rev. Environ. Econ. Policy* **2018**, *12*, 371–376. [[CrossRef](#)]
4. Winkler, K.; Fuchs, R.; Rounsevell, M.; Herold, M. Global Land Use Changes Are Four Times Greater than Previously Estimated. *Nat. Commun.* **2021**, *12*, 2501. [[CrossRef](#)]
5. Gilck, F.; Poschlod, P. The History of Human Land Use Activities in the Northern Alps since the Neolithic Age. A Reconstruction of Vegetation and Fire History in the Mangfall Mountains (Bavaria, Germany). *Holocene* **2021**, *31*, 579–591. [[CrossRef](#)]
6. McGowan, P.J.K. Conservation: Mapping the Terrestrial Human Footprint. *Nature* **2016**, *537*, 172–173. [[CrossRef](#)]
7. Chilukoti, N.; Xue, Y. An Assessment of Potential Climate Impact during 1948–2010 Using Historical Land Use Land Cover Change Maps. *Int. J. Climatol.* **2021**, *41*, 295–315. [[CrossRef](#)]
8. He, X.; Liang, J.; Zeng, G.; Yuan, Y.; Li, X. The Effects of Interaction between Climate Change and Land-Use/Cover Change on Biodiversity-Related Ecosystem Services. *Glob. Chall.* **2019**, *3*, 1800095. [[CrossRef](#)] [[PubMed](#)]
9. Yan, M.; Liu, J.; Wang, Z. Global Climate Responses to Land Use and Land Cover Changes over the Past Two Millennia. *Atmosphere* **2017**, *8*, 64. [[CrossRef](#)]
10. Pongratz, J.; Dolman, H.; Don, A.; Erb, K.H.; Fuchs, R.; Herold, M.; Jones, C.; Kuemmerle, T.; Luyssaert, S.; Meyfroidt, P.; et al. Models Meet Data: Challenges and Opportunities in Implementing Land Management in Earth System Models. *Glob. Chang. Biol.* **2018**, *24*, 1470–1487. [[CrossRef](#)]
11. Newbold, T.; Hudson, L.N.; Hill, S.L.L.; Contu, S.; Lysenko, I.; Senior, R.A.; Börger, L.; Bennett, D.J.; Choimes, A.; Collen, B.; et al. Global Effects of Land Use on Local Terrestrial Biodiversity. *Nature* **2015**, *520*, 45–50. [[CrossRef](#)] [[PubMed](#)]
12. Grimm, N.B.; Faeth, S.H.; Golubiewski, N.E.; Redman, C.L.; Wu, J.; Bai, X.; Briggs, J.M. Global Change and the Ecology of Cities. *Science* **2008**, *319*, 756–760. [[CrossRef](#)] [[PubMed](#)]
13. Findell, K.L.; Berg, A.; Gentine, P.; Krasting, J.P.; Lintner, B.R.; Malyshev, S.; Santanello, J.A.; Shevliakova, E. The Impact of Anthropogenic Land Use and Land Cover Change on Regional Climate Extremes. *Nat. Commun.* **2017**, *8*, 989. [[CrossRef](#)] [[PubMed](#)]

14. Hessel, A.E.; Anchukaitis, K.J.; Jelsema, C.; Cook, B.; Byambasuren, O.; Leland, C.; Nachin, B.; Pederson, N.; Tian, H.; Hayles, L.A. Past and Future Drought in Mongolia. *Sci. Adv.* **2018**, *4*, 1–8. [CrossRef]
15. Lamchin, M.; Lee, J.; Lee, W.; Lee, E.J.; Kim, M.; Lim, C.; Choi, H.; Kim, S.-R. Assessment of Land Cover Change and Desertification Using Remote Sensing Technology in a Local Region of Mongolia. *Adv. Sp. Res.* **2015**, *57*, 64–77. [CrossRef]
16. Tsalis, T.A.; Malamateniou, K.E.; Koulouriotis, D.; Nikolaou, I.E. New Challenges for Corporate Sustainability Reporting: United Nations' 2030 Agenda for Sustainable Development and the Sustainable Development Goals. *Corp. Soc. Responsib. Environ. Manag.* **2020**, *27*, 1617–1629. [CrossRef]
17. Liang, X.; Li, P.; Wang, J.; Chan, F.K.S.; Togtokh, C.; Ochir, A.; Davaasuren, D. Research Progress of Desertification and Its Prevention in Mongolia. *Sustainability* **2021**, *13*, 6861. [CrossRef]
18. FROM-GLC (10–30 m, 2015, 2017, China). Available online: <http://data.ess.tsinghua.edu.cn/> (accessed on 3 February 2022).
19. Esri Land Cover (10 m, 2017–2021, ESA). Available online: <https://www.esri.com/en-us/home> (accessed on 3 February 2018).
20. Globe Land 30 (30 m, 2000, 2010, 2020, China). Available online: <http://data.ess.tsinghua.edu.cn/> (accessed on 3 February 2022).
21. Global Land Survey (30 m, 1975–2012, USGS). Available online: <https://www.usgs.gov/> (accessed on 3 February 2022).
22. Climate Change Initiative Land Cover V2 (300 m, 1992–2020, ESA). Available online: <https://www.esa-landcover-cci.org/> (accessed on 3 February 2022).
23. MODIS Land Cover Type/Dynamics (0.5–1 Km, 2001–2020, NASA). Available online: <https://lpdaac.usgs.gov> (accessed on 3 February 2022).
24. Xu, L.; Herold, M.; Tsendbazar, N.-E.; Masiliunas, D.; Li, L.; Lesiv, M.; Fritz, S.; Verbesselt, J. Time Series Analysis for Global Land Cover Change Monitoring: A Comparison across Sensors. *Remote Sens. Environ.* **2022**, *271*, 112905. [CrossRef]
25. Nasiri, V.; Deljouei, A.; Moradi, F.; Sadeghi, S.; Moein, M.; Borz, S.A. Land Use and Land Cover Mapping Using Sentinel-2, Landsat-8 Satellite Images, and Google Earth Engine: A Comparison of Two Composition Methods. *Remote Sens.* **2022**, *14*, 1977. [CrossRef]
26. Choi, M.J.; Enkhbat, U. Distributional Effects of Ger Area Redevelopment in Ulaanbaatar, Mongolia. *Int. J. Urban Sci.* **2020**, *24*, 50–68. [CrossRef]
27. Wei, Y.; Zhen, L.; Liu, X.; Batkhishig, O. Land Use Change and Its Driving Factors in Mongolia from 1992 to 2005. *Chin. J. Appl. Ecol.* **2008**, *19*, 1995–2002. [CrossRef]
28. Vittek, M.; Brink, A.; Donnay, F.; Simonetti, D.; Desclée, B. Land Cover Change Monitoring Using Landsat MSS/TM Satellite Image Data over West Africa between 1975 and 1990. *Remote Sens.* **2013**, *6*, 658–676. [CrossRef]
29. Liu, S.; Liu, X.; Yu, L.; Wang, Y.; Zhang, G.J.; Gong, P.; Huang, W.; Wang, B.; Yang, M.; Cheng, Y. Climate Response to Introduction of the ESA CCI Land Cover Data to the NCAR CESM. *Clim. Dyn.* **2021**, *56*, 4109–4127. [CrossRef]
30. Ersi, C.; Bayaer, T.; Bao, Y.; Bao, Y.; Yong, M.; Zhang, X. Temporal and Spatial Changes in Evapotranspiration and Its Potential Driving Factors in Mongolia over the Past 20 Years. *Remote Sens.* **2022**, *14*, 1856. [CrossRef]
31. Li, G.; Wang, J.; Wang, Y.; Wei, H.; Ochir, A.; Davaasuren, D.; Chonokhuu, S.; Nasanbat, E. Spatial and Temporal Variations in Grassland Production from 2006 to 2015 in Mongolia along the China-Mongolia Railway. *Sustainability* **2019**, *11*, 2177. [CrossRef]
32. Tsalis, T.A.; Malamateniou, K.E.; Koulouriotis, D.; Nikolaou, I.E. Land Cover Change Analysis to Assess Sustainability of Development in the Mongolian Plateau over 30 Years. *Sustainability* **2022**, *14*, 6129. [CrossRef]
33. Wang, J.; Cheng, K.; Liu, Q.; Zhu, J.; Ochir, A.; Davaasuren, D.; Li, G.; Wei, H.; Chonokhuu, S.; Namsrai, O.; et al. Land Cover Patterns in Mongolia and Their Spatiotemporal Changes from 1990 to 2010. *Arab. J. Geosci.* **2019**, *12*, 1–13. [CrossRef]
34. Ma, L.; Li, M.; Ma, X.; Cheng, L.; Du, P.; Liu, Y. A Review of Supervised Object-Based Land-Cover Image Classification. *ISPRS J. Photogramm. Remote Sens.* **2017**, *130*, 277–293. [CrossRef]
35. Xie, T.; Yuan, Z.; Yang, H.; Jiang, M.; Liao, Z.; Xu, C. Review of Land Use/Cover Change Classification Methods Based on Remote Sensing Image. *Front. Earth Sci.* **2020**, *10*, 500–507. [CrossRef]
36. Hassan Khavarian Nehzak, M.A.; Mostafazadeh, R. Hamidreza Rabiei-Dastjerdi Chapter 5 - Assessment of Machine Learning Algorithms in Land Use Classification, *Comput. Earth Environ. Sci.* **2022**, 97–104. [CrossRef]
37. Alshari, E.A.; Gawali, B.W. Development of Classification System for LULC Using Remote Sensing and GIS. *Glob. Transitions Proc.* **2021**, *2*, 8–17. [CrossRef]
38. Ettehadi Osgouei, P.; Kaya, S. Analysis of Land Cover/Use Changes Using Landsat 5 TM Data and Indices. *Environ. Monit. Assess.* **2017**, *189*, 1–11. [CrossRef]
39. Rivera, S.; Lowry, J.H.; Hernandez, A.J.; Ramsey, R.D.; Lezama, R.; Velasquez, M.A. A Comparison between Cluster Busting Technique and a Classification Tree Algorithm of a Moderate Resolution Imaging Spectrometer (MODIS) Land Cover Map of Honduras. *Geocarto Int.* **2012**, *27*, 17–29. [CrossRef]
40. Sang, X.; Guo, Q.; Wu, X.; Fu, Y.; Xie, T.; He, C.; Zang, J. Intensity and Stationarity Analysis of Land Use Change Based on CART Algorithm. *Sci. Rep.* **2019**, *9*, 12279. [CrossRef] [PubMed]
41. Gislason, P.O.; Benediktsson, J.A.; Sveinsson, J.R. Random Forests for Land Cover Classification. *Pattern Recognit. Lett.* **2006**, *27*, 294–300. [CrossRef]
42. Nguyen, L.H.; Joshi, D.R.; Clay, D.E.; Henebry, G.M. Characterizing Land Cover/Land Use from Multiple Years of Landsat and MODIS Time Series: A Novel Approach Using Land Surface Phenology Modeling and Random Forest Classifier. *Remote Sens. Environ.* **2020**, *238*. [CrossRef]

43. Spinoni, J.; Barbosa, P.; Bucchignani, E.; Cassano, J.; Cavazos, T.; Cescatti, A.; Christensen, J.H.; Christensen, O.B.; Coppola, E.; Evans, J.P.; et al. Global Exposure of Population and Land-Use to Meteorological Droughts under Different Warming Levels and SSPs: A CORDEX-Based Study. *Int. J. Climatol.* **2021**, *41*, 6825–6853. [CrossRef]
44. Sakamoto, K.; Tomonari, M.; Ariya, U.; Nakagiri, E.; Matsumoto, T.K.; Akaji, Y.; Otoda, T.; Hirobe, M.; Nachin, B. Effects of Large-Scale Forest Fire Followed by Illegal Logging on the Regeneration of Boreal Forests in Mongolia. *Landsc. Ecol. Eng.* **2021**, *17*, 267–279. [CrossRef]
45. Xu, Y.; Zhang, Y.; Chen, J.; John, R. Livestock Dynamics under Changing Economy and Climate in Mongolia. *Land Use Policy* **2019**, *88*, 104120. [CrossRef]
46. Mandakh, N.; Tsogtbaatar, J.; Dash, D.; Khudulmur, S. Spatial Assessment of Soil Wind Erosion Using WEQ Approach in Mongolia. *J. Geogr. Sci.* **2016**, *26*, 473–483. [CrossRef]
47. Li, Y.; Wang, J.; Zhu, J. Landscape Pattern Analysis of Mongolia Based on the Geographical Partitions. *Arid L. Geogr.* **2016**, *39*, 817–827.
48. Wang, J.; Wei, H.; Cheng, K.; Ochir, A.; Shao, Y.; Yao, J.; Wu, Y.; Han, X.; Davaasuren, D.; Chonokhuu, S.; et al. Updatable Dataset Revealing Decade Changes in Land Cover Types in Mongolia. *Geosci. Data J.* **2022**, *9*, 341–354. [CrossRef]
49. Sanzheev, E.D.; Mikheeva, A.S.; Osodoev, P.V.; Batomunkuev, V.S.; Tulokhonov, A.K. Theoretical Approaches and Practical Assessment of Socio-Economic Effects of Desertification in Mongolia. *Int. J. Environ. Res. Public Health* **2020**, *17*, 4068. [CrossRef] [PubMed]
50. Wang, J.; Wei, H.; Cheng, K.; Ochir, A.; Davaasuren, D.; Li, P.; Shun Chan, F.K.; Nasanbat, E. Spatio-Temporal Pattern of Land Degradation from 1990 to 2015 in Mongolia. *Environ. Dev.* **2020**, *34*, 100497. [CrossRef]
51. The Climate in Mongolia. Available online: <https://www.worlddata.info/asia/mongolia/climate.php> (accessed on 3 February 2018).
52. Vandandorj, S.; Munkhjargal, E.; Boldgiv, B.; Gantsetseg, B. Changes in Event Number and Duration of Rain Types over Mongolia from 1981 to 2014. *Environ. Earth Sci.* **2017**, *76*, 70. [CrossRef]
53. Dugarsuren, N.; Lin, C.; Tsogt, H. Land Cover Change Detection in Mongolia in Last Decade Using Modis Imagery. *Remote Sens.* **2011**, *4*, 2750–2755.
54. Punsantsogvoov, T. Implications of Rural Settlement Patterns for Development: Case Study in Central and Eastern Economic Region of Mongolia. *Proc. Mong. Acad. Sci.* **2019**, *59*, 14–20. [CrossRef]
55. Map Cruzin Data Research & GIS Project Specialist. Available online: <https://mapcruzin.com/> (accessed on 1 May 2022).
56. Fang, X.; Zhao, W.; Zhang, C.; Zhang, D.; Wei, X.; Qiu, W.; Ye, Y. Methodology for Credibility Assessment of Historical Global LUCC Datasets. *Sci. China Earth Sci.* **2020**, *63*, 1013–1025. [CrossRef]
57. Soni, P.K.; Rajpal, N.; Mehta, R.; Mishra, V.K. Urban Land Cover and Land Use Classification Using Multispectral Sentinel-2 Imagery. *Multimed. Tools Appl.* **2022**, *81*, 36853–36867. [CrossRef]
58. Gorelick, N.; Hancher, M.; Dixon, M.; Ilyushchenko, S.; Thau, D.; Moore, R. Google Earth Engine: Planetary-Scale Geospatial Analysis for Everyone. *Remote Sens. Environ.* **2017**, *202*, 18–27. [CrossRef]
59. Mas, J.F.; de Araújo, F.S. Assessing Landsat Images Availability and Its Effects on Phenological Metrics. *Forests* **2021**, *12*, 574. [CrossRef]
60. Cao, R.; Feng, Y.; Chen, J.; Zhou, J. A Supplementary Module to Improve Accuracy of the Quality Assessment Band in Landsat Cloud Images. *Remote Sens.* **2021**, *13*, 4947. [CrossRef]
61. Li, G.; Sun, S.; Fang, C. The Varying Driving Forces of Urban Expansion in China: Insights from a Spatial-Temporal Analysis. *Landsc. Urban Plan.* **2018**, *174*, 63–77. [CrossRef]
62. Wu, X.; Liu, H.; Li, X.; Piao, S.; Ciais, P.; Guo, W.; Yin, Y.; Poulter, B.; Peng, C.; Viovy, N.; et al. Higher Temperature Variability Reduces Temperature Sensitivity of Vegetation Growth in Northern Hemisphere. *Geophys. Res. Lett.* **2017**, *44*, 6173–6181. [CrossRef]
63. Li, X.; Guo, W.; Chen, J.; Ni, X.; Wei, X. Responses of Vegetation Green-up Date to Temperature Variation in Alpine Grassland on the Tibetan Plateau. *Ecol. Indic.* **2019**, *104*, 390–397. [CrossRef]
64. Hansson, A.; Dargusch, P.; Shulmeister, J. A Review of Modern Treeline Migration, the Factors Controlling It and the Implications for Carbon Storage. *J. Mt. Sci.* **2021**, *18*, 291–306. [CrossRef]
65. Bai, Y.; Wu, J.; Xing, Q.; Pan, Q.; Huang, J.; Yang, D.; Han, X. Primary Production and Rain Use Efficiency across a Precipitation Gradient on the Mongolia Plateau. *Ecology* **2008**, *89*, 2140–2153. [CrossRef]
66. Bai, W.; Wan, S.; Niu, S.; Liu, W.; Chen, Q.; Wang, Q.; Zhang, W.; Han, X.; Li, L. Increased Temperature and Precipitation Interact to Affect Root Production, Mortality, and Turnover in a Temperate Steppe: Implications for Ecosystem C Cycling. *Glob. Chang. Biol.* **2010**, *16*, 1306–1316. [CrossRef]
67. Miehe, G.; Schlütz, F.; Miehe, S.; Opgenoorth, L.; Cermak, J.; Samiya, R.; Jäger, E.J.; Wesche, K. Mountain Forest Islands and Holocene Environmental Changes in Central Asia: A Case Study from the Southern Gobi Altay, Mongolia. *Palaeogeogr. Palaeoclimatol. Palaeoecol.* **2007**, *250*, 150–166. [CrossRef]
68. Miao, H.; Chen, S.; Chen, J.; Zhang, W.; Zhang, P.; Wei, L.; Han, X.; Lin, G. Cultivation and Grazing Altered Evapotranspiration and Dynamics in Inner Mongolia Steppes. *Agric. For. Meteorol.* **2009**, *149*, 1810–1819. [CrossRef]
69. Horel, Á.; Zsigmond, T.; Farkas, C.; Gelybó, G.; Tóth, E.; Kern, A.; Bakacsi, Z. Climate Change Alters Soil Water Dynamics under Different Land Use Types. *Sustainability* **2022**, *14*, 3908. [CrossRef]

70. Berihun, M.L.; Tsunekawa, A.; Haregeweyn, N.; Meshesha, D.T.; Adgo, E.; Tsubo, M.; Masunaga, T.; Fenta, A.A.; Sultan, D.; Yibeltal, M. Exploring Land Use/Land Cover Changes, Drivers and Their Implications in Contrasting Agro-Ecological Environments of Ethiopia. *Land Use Policy* **2019**, *87*, 104052. [[CrossRef](#)]
71. Wu, F.; Mo, C.; Dai, X. Analysis of the Driving Force of Land Use Change Based on Geographic Detection and Simulation of Future Land Use Scenarios. *Sustainability* **2022**, *14*, 5254. [[CrossRef](#)]
72. Ruan, X.; Qiu, F.; Dyck, M. The Effects of Environmental and Socioeconomic Factors on Land-Use Changes: A Study of Alberta, Canada. *Environ. Monit. Assess.* **2016**, *188*, 1–31. [[CrossRef](#)]
73. Wang, Y.; Xia, T.; Shataer, R.; Zhang, S.; Li, Z. Analysis of Characteristics and Driving Factors of Land-Use Changes in the Tarim River Basin from 1990 to 2018. *Sustainability* **2021**, *13*, 10263. [[CrossRef](#)]
74. Wilkin, S.; Ventresca Miller, A.; Miller, B.K.; Spengler, R.N.; Taylor, W.T.T.; Fernandes, R.; Hagan, R.W.; Bleasdale, M.; Zech, J.; Ulziibayar, S.; et al. Economic Diversification Supported the Growth of Mongolia’s Nomadic Empires. *Sci. Rep.* **2020**, *10*, 3916. [[CrossRef](#)]
75. Wei, Y.; Zhen, L. The Dynamics of Livestock and Its Influencing Factors on the Mongolian Plateau. *Environ. Dev.* **2020**, *34*, 100518. [[CrossRef](#)]
76. Reguzzoni, M.; Carrion, D.; De Gaetani, C.I.; Albertella, A.; Rossi, L.; Sona, G.; Batsukh, K.; Herrera, J.F.T.; Elger, K.; Barzaghi, R.; et al. Open Access to Regional Geoid Models: The International Service for the Geoid. *Earth Syst. Sci. Data* **2021**, *13*, 1653–1666. [[CrossRef](#)]
77. Fu, Y.; Zhang, Y. Research on Temporal and Spatial Evolution of Land Use and Landscape Pattern in Anshan City Based on GEE. *Front. Environ. Sci.* **2022**, *10*, 1–17. [[CrossRef](#)]
78. Giles, M. Foody Status of Land Cover Classification Accuracy Assessment. *Remote Sens. Environ.* **2002**, *80*, 185–201. [[CrossRef](#)]
79. Paul, A.; Mukherjee, D.P.; Member, S.; Das, P.; Gangopadhyay, A. Improved Random Forest for Classification. *IEEE Trans. Image Process.* **2018**, *27*, 7149, 1–13. [[CrossRef](#)]
80. Naikoo, M.W.; Talukdar, S.; Ishtiaq, M.; Rahman, A. Modelling Built-up Land Expansion Probability Using the Integrated Fuzzy Logic and Coupling Coordination Degree Model. *J. Environ. Manag.* **2023**, *325*, 116441. [[CrossRef](#)] [[PubMed](#)]
81. Belgiu, M.; Drăgu, L. Random Forest in Remote Sensing: A Review of Applications and Future Directions. *ISPRS J. Photogramm. Remote Sens.* **2016**, *114*, 24–31. [[CrossRef](#)]
82. Ghorbanian, A.; Zaghian, S.; Asiyabi, R.M.; Amani, M.; Mohammadzadeh, A.; Jamali, S. Mangrove Ecosystem Mapping Using Sentinel-1 and Sentinel-2 Satellite Images and Random Forest Algorithm in Google Earth Engine. *Remote Sens.* **2021**, *13*, 2565. [[CrossRef](#)]
83. Cui, J.; Zhu, M.; Liang, Y.; Qin, G.; Li, J.; Liu, Y. Land Use/Land Cover Change and Their Driving Factors in the Yellow River Basin of Shandong Province Based on Google Earth Engine from 2000 to 2020. *ISPRS Int. J. Geo-Information* **2022**, *11*, 163. [[CrossRef](#)]
84. Zhang, D.D.; Zhang, L. Land Cover Change in the Central Region of the Lower Yangtze River Based on Landsat Imagery and the Google Earth Engine: A Case Study in Nanjing, China. *Sensors* **2020**, *20*, 2091. [[CrossRef](#)]
85. Liu, C.; Li, W.; Zhu, G.; Zhou, H.; Yan, H.; Xue, P. Land Use/Land Cover Changes and Their Driving Factors in the Northeastern Tibetan Plateau Based on Geographical Detectors and Google Earth Engine: A Case Study in Gannan Prefecture. *Remote Sens.* **2020**, *12*, 3139. [[CrossRef](#)]
86. Fitoka, E.; Tompoulidou, M.; Hatziiordanou, L.; Apostolakis, A.; Höfer, R.; Weise, K.; Ververis, C. Water-Related Ecosystems’ Mapping and Assessment Based on Remote Sensing Techniques and Geospatial Analysis: The SWOS National Service Case of the Greek Ramsar Sites and Their Catchments. *Remote Sens. Environ.* **2020**, *245*, 111795. [[CrossRef](#)]
87. Zhang, M.; Du, H.; Mao, F.; Zhou, G.; Li, X.; Dong, L.; Zheng, J.; Zhu, D.; Liu, H.; Huang, Z.; et al. Spatiotemporal Evolution of Urban Expansion Using Landsat Time Series Data and Assessment of Its Influences on Forests. *ISPRS Int. J. Geo-Information* **2020**, *9*, 64. [[CrossRef](#)]
88. Ghulam, A. Monitoring Tropical Forest Degradation in Betampona Nature Reserve, Madagascar Using Multisource Remote Sensing Data Fusion. *IEEE J. Sel. Top. Appl. Earth Obs. Remote Sens.* **2014**, *7*, 4960–4971. [[CrossRef](#)]
89. Zou, D.; Zhao, L.; Liu, G.; Du, E.; Hu, G.; Li, Z.; Wu, T.; Wu, X.; Chen, J. Vegetation Mapping in the Permafrost Region: A Case Study on the Central Qinghai-Tibet Plateau. *Remote Sens.* **2022**, *14*, 232. [[CrossRef](#)]
90. Cheng, K.; Wang, J. Forest Type Classification Based on Integrated Spectral-Spatial-Temporal Features and Random Forest Algorithm—A Case Study in the Qinling Mountains. *Forests* **2019**, *10*, 559. [[CrossRef](#)]
91. Wickham, J.; Stehman, S.V.; Gass, L.; Dewitz, J.A.; Sorenson, D.G.; Granneman, B.J.; Poss, R.V.; Baer, L.A. The-matic Accuracy Assessment of the 2011 National Land Cover Database (NLCD). *Remote Sens. Environ.* **2017**, *191*, 328–341. [[CrossRef](#)] [[PubMed](#)]
92. Pontius, R.G.; Huang, J.; Jiang, W.; Khallaghi, S.; Lin, Y.; Liu, J.; Quan, B.; Ye, S. Rules to Write Mathematics to Clarify Metrics Such as the Land Use Dynamic Degrees. *Landsc. Ecol.* **2017**, *32*, 2249–2260. [[CrossRef](#)]
93. Jun, C.; Ban, Y.; Li, S. Open Access to Earth Land-Cover Map. *Nature* **2014**, *514*, 434. [[CrossRef](#)]
94. Pluto-Kossakowska, J. Review on Multitemporal Classification Methods of Satellite Images for Crop and Arable Land Recognition. *Agriculture* **2021**, *11*, 999. [[CrossRef](#)]
95. Li, M.; Li, X.; Liu, S.; Lyu, X.; Dang, D.; Dou, H.; Wang, K. Analysis of the Spatiotemporal Variation of Landscape Patterns and Their Driving Factors in Inner Mongolia from 2000 to 2015. *Land* **2022**, *11*, 1410. [[CrossRef](#)]
96. Li, J.; Chen, H.; Zhang, C.; Pan, T. Variations in Ecosystem Service Value in Response to Land Use/Land Cover Changes in Central Asia from 1995–2035. *PeerJ* **2019**, *7*, e7665. [[CrossRef](#)]

97. Henchiri, M.; Ali, S.; Essifi, B.; Kalisa, W.; Zhang, S.; Bai, Y. Monitoring Land Cover Change Detection with NOAA-AVHRR and MODIS Remotely Sensed Data in the North and West of Africa from 1982 to 2015. *Environ. Sci. Pollut. Res.* **2020**, *27*, 5873–5889. [[CrossRef](#)]
98. De Rosa, M.; Vestergaard Odgaard, M.; Staunstrup, J.K.; Trydeman Knudsen, M.; Hermansen, J.E. Identifying Land Use and Land-Use Changes (LULUC): A Global LULUC Matrix. *Environ. Sci. Technol.* **2017**, *51*, 7954–7962. [[CrossRef](#)]
99. Qin, F.; Jia, G.; Yang, J.; Na, Y.; Hou, M.; Narenmandula. Spatiotemporal Variability of Precipitation during 1961–2014 across the Mongolian Plateau. *J. Mt. Sci.* **2018**, *15*, 992–1005. [[CrossRef](#)]
100. Yang, T.; Li, P.; Wu, X.; Hou, X.; Liu, P.; Yao, G. Assessment of Vulnerability to Climate Change in the Inner Mongolia Steppe at a County Scale from 1980 to 2009. *Rangel. J.* **2014**, *36*, 545–555. [[CrossRef](#)]
101. Bliedtner, M.; Strobel, P.; Struck, J.; Salazar, G.; Szidat, S.; Nowaczyk, N.; Bazarradnaa, E.; Lloren, R.; Dubois, N.; Haberzettl, T.; et al. Holocene Temperature Variations in Semi-Arid Central Mongolia—A Chronological and Sedimentological Perspective From a 7400-Year Lake Sediment Record From the Khangai Mountains. *Front. Earth Sci.* **2022**, *10*, 910782. [[CrossRef](#)]
102. Ojima, D.S.; Chuluun, T.; Bolortsetseg, B.; Tucker, C.J.; Hicke, J. Eurasian Land Use Impacts on Rangeland Productivity. *Geophys. Monogr. Ser.* **2004**, *153*, 293–301. [[CrossRef](#)]
103. Hilker, T.; Natsagdorj, E.; Waring, R.H.; Lyapustin, A.; Wang, Y. Satellite Observed Widespread Decline in Mongolian Grasslands Largely Due to Overgrazing. *Glob. Chang. Biol.* **2014**, *20*, 418–428. [[CrossRef](#)]
104. Yao, Z.; Zhang, L.; Tang, S.; Li, X.; Hao, T. The Basic Characteristics and Spatial Patterns of Global Cultivated Land Change since the 1980s. *J. Geogr. Sci.* **2017**, *27*, 771–785. [[CrossRef](#)]
105. Buyanduureng. Chelger Agglomeration and Regional Differences of the Mongolia’s Agricultural Industry Based on the Space Economics. *Inn. Mong. Soc. Sci.* **2017**, *38*, 184–189. [[CrossRef](#)]
106. Zandariya, B. Improving the Policy Framework for Financial Assurance for Mine Closure in Mongolia. *Resour. Policy* **2022**, *77*, 102628. [[CrossRef](#)]
107. Wang, Z.; Wang, H.; Wang, T.; Wang, L.; Liu, X.; Zheng, K.; Huang, X. Large Discrepancies of Global Greening: Indication of Multi-Source Remote Sensing Data. *Glob. Ecol. Conserv.* **2022**, *34*, e02016. [[CrossRef](#)]
108. Piao, S.; Wang, X.; Park, T.; Chen, C.; Lian, X.; He, Y.; Bjerke, J.W.; Chen, A.; Ciais, P.; Nemani, R.R.; et al. Characteristics, Drivers and Feedbacks of Global Greening Shilong. *Nat. Rev. Earth Environ.* **2019**, *1*, 14–27. [[CrossRef](#)]
109. D’Odorico, P.; Bhattachan, A.; Davis, K.F.; Ravi, S.; Runyan, C.W. Global Desertification: Drivers and Feedbacks. *Adv. Water Resour.* **2013**, *51*, 326–344. [[CrossRef](#)]
110. Funk, M.; Sugden, A.M. Degradation Exceeds Deforestation. *Science* **2013**, *369*, 1335–1336. [[CrossRef](#)]
111. Zhang, Y.; Wang, Q.; Wang, Z.; Yang, Y.; Li, J. Impact of Human Activities and Climate Change on the Grassland Dynamics under Different Regime Policies in the Mongolian Plateau. *Sci. Total Environ.* **2020**, *698*, 134304. [[CrossRef](#)]
112. Park, H.; Fan, P.; John, R.; Chen, J. Urbanization on the Mongolian Plateau after Economic Reform: Changes and Causes. *Appl. Geogr.* **2017**, *86*, 118–127. [[CrossRef](#)]
113. Dashpurev, B.; Bendix, J.; Lehnert, L.W. Monitoring Oil Exploitation Infrastructure and Dirt Roads with Object-Based Image Analysis and Random Forest in the Eastern Mongolian Steppe. *Remote Sens.* **2020**, *12*, 144. [[CrossRef](#)]
114. Krausmann, F.; Langthaler, E. Food Regimes and Their Trade Links: A Socio-Ecological Perspective. *Ecol. Econ.* **2019**, *160*, 87–95. [[CrossRef](#)]
115. Yekimovskaya, O.A.; Lopatina, D.N. The Features of Development of Agricultural Land Use in the Republic of Buryatia and Mongolia (the Selenga River Basin). *IOP Conf. Ser. Earth Environ. Sci.* **2019**, *320*, 012007. [[CrossRef](#)]
116. Shao, C.; Chen, J.; Li, L.; Dong, G.; Han, J.; Abraha, M.; John, R. Grazing Effects on Surface Energy Fluxes in a Desert Steppe on the Mongolian Plateau. *Ecol. Appl.* **2017**, *27*, 485–502. [[CrossRef](#)]
117. Jin, L.; Zhang, J.; Wang, R.; Zhang, M.; Bao, Y.; Guo, E.; Wang, Y. Analysis for Spatio-Temporal Variation Characteristics of Droughts in Different Climatic Regions of the Mongolian Plateau Based on SPEI. *Sustainability* **2019**, *11*, 5767. [[CrossRef](#)]
118. Meng, X.; Gao, X.; Li, S.; Li, S.; Lei, J. Monitoring Desertification in Mongolia Based on Landsat Images and Google Earth Engine from 1990 to 2020. *Ecol. Indic.* **2021**, *129*, 107908. [[CrossRef](#)]
119. Kimura, R.; Moriyama, M. Use of a Modis Satellite-Based Aridity Index to Monitor Drought Conditions in Mongolia from 2001 to 2013. *Remote Sens.* **2021**, *13*, 2561. [[CrossRef](#)]

**Disclaimer/Publisher’s Note:** The statements, opinions and data contained in all publications are solely those of the individual author(s) and contributor(s) and not of MDPI and/or the editor(s). MDPI and/or the editor(s) disclaim responsibility for any injury to people or property resulting from any ideas, methods, instructions or products referred to in the content.